JOURNAL OF MATERIALS SCIENCE 17 (1982) 2066–2106

An investigation of material variables of epoxy resins controlling transverse cracking in composites

SHAW MING LEE, RICHARD D. SCHILE
CIBA-GEIGY Corporation, Composite Products Research, Ardsley, NY 10502, USA

Residual stresses in curing resins in laminates were successfully measured with a unique testing technique. Residual stresses at least of the same order of magnitude as the tensile strength of the resin were built up as a result of resin shrinkage induced by chemical reaction and the thermal mismatch between fibre and resin both above the glass transition temperature, and below. Residual stresses can be reduced if the resin can be almost fully cured at a relatively low temperature and further post-cure will not activate appreciable additional reaction. Fracture toughness tests were also carried out on cast resin samples. High resin fracture-toughness and low resin residual stress are the conditions desired for the laminate to resist transverse cracking. Although this ideal combination was not realized for the resin systems in our study, it should be achievable once the curing cycle as well as the resin formulation are properly adjusted.

1. Introduction

Transverse cracking is a major type of damage frequently observed in fibre-reinforced laminates. The damage consists of multiple transverse cracks in plies resulting from the applied load perpendicular to the fibre direction of the plies. The cracks usually occur at a relatively low load level, well before the full load capacity of the fibres is reached. The damage can sometimes lead to catastrophic failure of the laminates but usually results in laminate property degradation. For instance, transverse cracking can cause weepage in filament-wound pressure vessels at low pressure level. In all cases, this type of damage is detrimental to structural reliability and durability.

Transverse cracking is a matrix-dominated failure process. When a ply is under transverse loading, most of the strain is concentrated in the thin layer of resin between the fibres. The fibres, much stronger and stiffer than the resin, are seldom fractured by this type of applied load. It is, therefore, germane to study the important resin material variables controlling transverse cracking because this information is crucial to the selection of resins for laminate applications.

There has been a fair amount of work [1-7] addressing the macromechanical behaviour of transverse cracking. Although there is a good understanding of the effective transverse cracking properties of the ply, treated as a homogeneous material, the resin material properties contributing to the failure process still remain unclear. The correlation between the resin material properties and the laminate transverse cracking behaviour has commonly been established in a qualitative manner [8–10] since the stress state in the resin of the laminate is too complicated to be accurately accounted for. The ascription of the laminate performance to the simple tensile stress–strain behaviour of the resin may not be conclusive. The resin, under the triaxial stress state in the laminate will behave differently from the uniaxial stress state in simple tension [11]. It appears that a good correlation requires the identification of relevant material variables governing the failure process as well as micromechanical study to predict the possible *in situ* failure process.

The purpose of this work was to study the important resin material variables controlling the transverse cracking process. Our attention has been focused on two critical resin properties: the resin residual stress in the cured laminate and the

0022–2461/82/072095–12$03.94/0

fracture-toughness of the resin. The failure process of transverse cracking has been shown [6, 7] to be a function of the fracture-toughness of the ply. The ply fracture-toughness, in turn, is a strong function of the fracture-toughness of the resin. The residual stress in the resin in a laminate, on the other hand, is built up during the curing cycle because of:

(a) the resin shrinkage induced by chemical reactions;

(b) the thermal misfit during cooling between fibres and matrix; and

(c) the constraints between laminae oriented in different directions. This residual stress is a function of the resin type, the curing process and the laminate arrangement. Its level has been measured in this study to be at least of the same order of magnitude as the tensile strength of the resin. Although the non-uniform and triaxial residual stress distribution may not immediately cause failure of the laminate, it will undoubtedly induce microdamage such as cracks and crazes. Therefore, the existence of residual stresses certainly reduces the structural integrity, especially the matrix-sensitive transverse strength of the laminate.

In this study, several epoxy resin systems were characterized by measuring their fracture toughness and residual stress level. A unique technique for measuring the residual stress build-up in the resin was developed using an array of glass rods embedded in the resin to simulate the fibre–matrix structure in the laminate. The central glass rod in the array was instrumented with strain gauges and a temperature sensor to yield the residual stress build-up and curing history. In addition, fracture-toughness tests were carried out on cast resin samples. Valuable information on the residual stress build-up as well as on the importance of the residual stress in conjunction with the fracture-toughness in controlling the transverse cracking behaviour was gathered as a result of this study.

2. Experimental details

2.1. Materials description

A variety of CIBA-GEIGY epoxy resin–hardener systems were selected for this study. Not all of the resin systems chosen are currently being used for laminate applications. However, they all have distinct fracture-toughness and residual stress build-up characteristics.

For each resin system, fracture-toughness and residual stress build-up samples were cured in the same curing cycle which corresponded, whenever possible, to the laminate curing process. The purpose was to prepare resin samples that best represented the matrix materials in the real laminates. The materials used in this work are listed in Table I and the resin systems and their curing cycles are given in Table II. These resins were prepared by mixing and degassing the resin–hardener mixtures under vacuum in a 3-neck flask. In most cases, the mixing procedures specified in the CIBA-GEIGY epoxy resin catalogue for resin casting were followed. When accelerator was used, extra care was taken to prevent accidental advancing of the resin system.

2.2. Residual strain measurements

2.2.1. Test method

Up to the present time the measurements of residual stress in the polymeric resin of a laminate has been an impossible task. In a real laminate, the fibres are not only quite small but also closely spaced. There is simply not a large enough space in the resin for any existing instrumentation. It is, however, possible to measure the residual stress in indirect ways. According to elasticity theory, two continuous bodies of the same material and geometry but of different sizes, when under the same imposed strain field, will have the same stress distribution at their corresponding relative points. This means that if the fibres in a laminate can be replaced with fibres of the same material of much

TABLE I Details of materials used in the investigation

Material Code	Type of material	Material
6010	Epoxy resin	Diglycidyl ether of bisphenol A (DGEBA)
906	Hardner	Methyl nadic anhydride (MNA)
HY 917	Hardner	Methyltetrahydrophthalic anhydride (MTHPA)
972	Hardner	Methylene dianiline (MDA)
PACM 20	Hardner	Bis(*p*-aminocyclohexyl) methane (a DuPont product)
062	Accelerator	Benzyl dimethylamine (BDMA)
064	Accelerator	Tri(dimethylaminomethyl) phenol

TABLE II The resin systems and their curing cycles

Epoxy resin/hardener(/accelerator) system	Weight ratio	Curing cycle
6010/972	100:27	100° C for 1 h → 150° C for 2 h → cool to room temperature
6010/906/064	100:80:3	150° C for 2.5 h → 177° C for 1 h → cool to room temperature
6010/HY 917/062	100:80:1	177° C for 3 h → cool to room temperature
6010/PACM 20/972	100:8.1:18.9	80° C for 1.5 h → 120° C for 1.5 h → 177° C for 1 h → cool to room temperature

larger size while still maintaining their relative positions, the stress field developed in the new laminate should be an exact mapping of that in the original laminate. Based on this argument, a new measurement technique was developed by casting epoxy resins with glass rods to simulate glass-fibre–epoxy laminates. The circular Pyrex glass rods of 7 mm diameter were chosen so that one of the rods could be instrumented with strain gauges and a temperature sensor. Two strain gauges (aquired from Micro-Measurements, SK-03-031CF-350) were mounted one axially and one transversely on the glass rod, as shown in Fig. 1. The output of these strain gauges was used to monitor the residual stress development in the resin during the entire cure and post-cure. The stress in the resin was proportional to the residual strain in the glass rod as determined by the attached strain gauges. The termperature sensor, on the other hand, provided the entire temperature history of the curing cycle.

During initial feasibility studies, a single instrumented glass rod was embedded in a curing neat-resin sample in a cylindrical can. The measurement of residual strains in the glass rod was proven practical by this test. However, the high exotherm (as high as 165° C above the intended curing temperature) in this large sample did not accurately represent the conditions experienced in a curing laminate. A few samples shattered during the final cooling because of the excess thermal misfit stresses.

An improved test with a regular, hexagonal array of glass rods embedded in resins cured in a dog-bone shaped steel mould, as shown in Fig. 2, was successfully developed to measure the residual

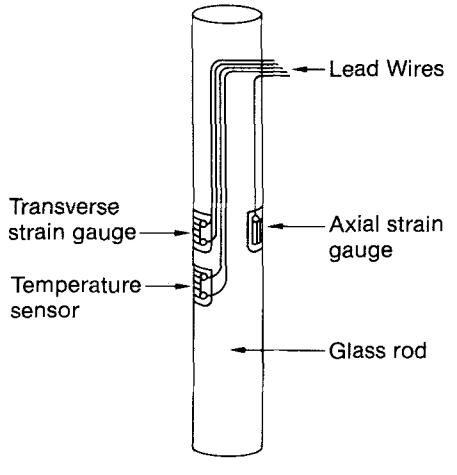

Figure 1 Schematic diagram of a glass rod mounted with an axial strain gauge, a transverse strain gauge and a temperature sensor.

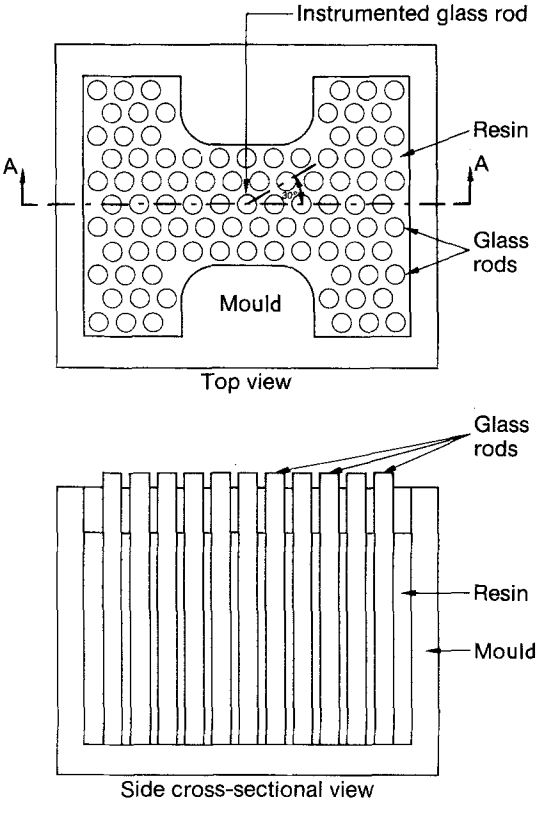

Figure 2 Schematic diagram of the dog-bone shaped sample in the mould used for the residual stress build-up measurements.

stress build-up in the resin through an instrumented, central rod. The volume content of glass rods in the sample was chosen to be 65%, approximately equal to that of the glass fibres in a typical composite, in order to more accurately reproduce the fibre arrangement in a real composite. The mould shape was intended to prevent the sample from contracting in the longitudinal direction, thus simulating the constraint imposed by the longitudinal plies in a laminate upon the transverse plies. The hoop strain gauge on the central rod was oriented in a direction 30° off the longitudinal axis of the mould, facing the resin-rich area, as shown in Fig. 2. The miniature strain gauge used occupied an arc of only 13° in the circumference of the glass rod. The mould was heated by contact heating pads with a feed-back temperature control. The exotherm of the samples was reduced to within 20° C above the heater temperature by the large volume of glass rods which helped to absorb heat during curing of the resins.

It was found however, that after a residual stress measurement was completed, the disassembly of the mould did not bring about the expected reduction of the stress already in the sample. It was then concluded that the specimen geometry was not effective in achieving the intended interlaminar constraint conditions. Further modification of the mould design for the purpose of constraining the sample, if needed, can perhaps be based on a photoelastic study or a finite element analysis. The residual stress measured with the existing mould, nevertheless, is meaningful in the sense that it provides fundamental information about the residual stress in an unconstrained, unidirectional ply. Even in a cross-ply laminate, this information is essential in distinguishing this residual stress component from that induced by the interlaminar constraint.

Although the photoelastic technique [12, 13] has been used to measure the residual stress field in the resin of a composite, the present technique does have several advantages. First, the residual stress build-up history can be recorded throughout the entire resin cure cycle. Second, this technique is applicable to resin systems which are not necessarily optically clear, as required for photoelastic analysis.

2.2.2. Specimen preparation and instrumentation

The strain gauges and the temperature sensors were bonded to the glass rods by using an epoxy-phenolic adhesive, M-Bond 610, supplied by Micro-Measurements. After bonding, the adhesive was cured at 177° C for 2 h and post-cured at 260° C for 3 h. The adhesive had a range of operating temperature from −269° C to 260° C (up to 370° C for short-term use). The bond line thickness was specified to be less than 0.005 mm.

The signals from the strain gauges and temperature sensors were conditioned by a Vishay 2300 multi-channel Signal Conditioning System. A Hewlett-Packard 3052 Data Acquisition System controlled by a Hewlett-Packard 9835 computer was used to record and process the data.

Before each test, the strain gauges bonded to the glass rod were calibrated for the strain, ϵ_g, due to the change in resistivity of the gauge with temperature as well as due to the difference in thermal expansion coefficients between the gauges and the rod. The instrumented rod was heated in an oven to a temperature above the intended post-cure temperature. The strain data, ϵ_g, so induced as a function of temperature, T, were fitted by a third-power polynomial by using a least-square fit method such that

$$\epsilon_g(T) = A + B(T - T_0) + C(T - T_0)^2 + D(T - T_0)^3, \quad (1)$$

where A, B, C and D are constants and T_0 is a reference temperature. A typical plot of ϵ_g against T is shown in Fig. 3. The reproducibility of the calibration curves was quite good.

During the test, the strain gauge output, ϵ_a (apparent strain), was composed of two components: ϵ_g and the residual strain, ϵ_R, induced by the deformation interaction between the resin and the glass, i.e.,

$$\epsilon_a = \epsilon_g + \epsilon_R. \quad (2)$$

The residual strain, ϵ_R, as a function of temperature was recorded automatically in the data acquisition system by subtracting ϵ_g from the directly measured ϵ_a.

2.3. Fracture-toughness tests

The compact tension and the three-point bend specimens recommended by ASTM [14, 15] for plane-strain fracture-toughness tests were employed in our attempt to characterize the epoxy resins listed in Table II. Both specimens were found to yield comparable results. The specimens were cut

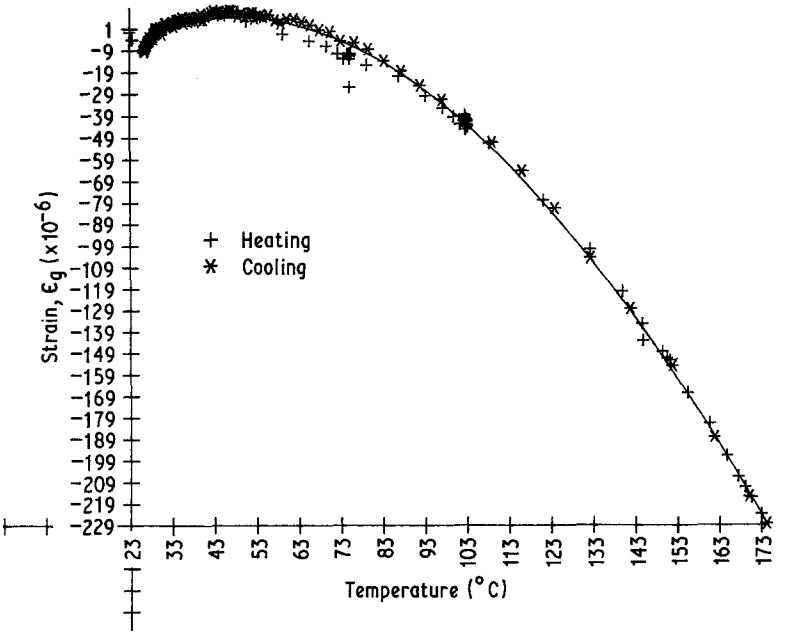

Figure 3 A typical calibration plot of strain, ϵ_g, against temperature, for a strain gauge bonded to a glass rod.

from cast neat-resin plates of 0.64 cm and 1.27 cm thicknesses. Cracks in the specimens were carefully introduced by first slotting the samples with a diamond abrasive saw and then tapping in a razor-blade at the slot roots to achieve a fine natural crack. All specimens were tested in an Instron machine at a cross-head speed of 0.05 cm min^{-1}.

2.4. Other tests

Compression tests were carried out on rectangular cross-section specimens (1.27 cm x 1.27 cm x 3 cm) cut from cast neat-resin plates. All specimens were instrumented with strain gauges so that their stress–strain relationship could be recorded. The initial slope of the stress–strain curve gave the Young's modulus of the resin, which should be very close to that obtained under tension. Another variable measured during the compression test was the yield stress of the resin, defined by the stress level at which the stress–strain curve started to level off (shown in Fig. 4). The yield stress reflected the ease with which the resin was able to undergo plastic deformation: an energy absorbing mechanism. The tests were carried out in an Instron machine at a cross-head speed of 0.05 cm min^{-1}.

The glass transition temperature, T_g, and the thermal expansion coefficient, α, of the resins were measured using a DuPont 942 Thermo Mechanical Analyser (TMA). The samples, cut from the cast epoxy plates, were then scanned in nitrogen environment at a scanning rate of 5° C min^{-1}. The linear dimension, l, of the specimens was recorded as a function of temperature, T. The thermal expansion coefficient, α, was defined as

$$\alpha = \frac{1}{l_0}\frac{dl}{dT}, \tag{3}$$

where l_0 was the original length of the sample. A typical thermal expansion curve had a break in linearity of the curve. This break point defined the glass transition temperature, T_g.

3. Numerical analysis

The strain measured in the tests using multiple glass rods in the dog-bone shaped sample described

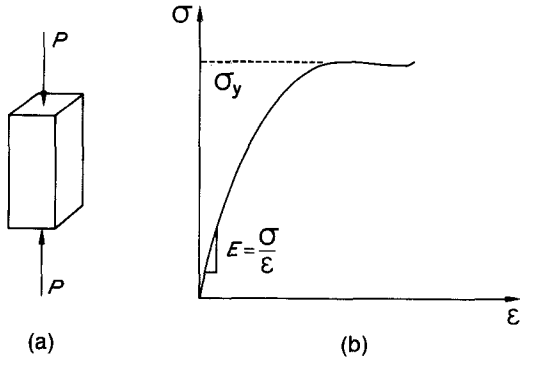

Figure 4 Uniaxial compression test. (a) Rectangular cross-section specimen, (b) stress–strain curve showing the elastic modulus, E, and the yield stress, σ_y.

earlier was that in the glass rod induced by the residual stress in the resin. The residual stress in the resin, assumed to be elastic, is derivable from the measured strain in the glass rod. Although a closed-form elasticity solution is hard to obtain, numerical schemes such as the finite-element method can be readily adopted to find a reasonably accurate stress distribution.

A NASTRAN finite-element computer program was employed to solve the two-dimensional, plane-strain problem involving a hexagonal array of glass rods embedded in the resin matrix subjected to a temperature change which induces thermal misfit. For an unconstrained unidirectional ply, the problem outlined can be reduced by symmetry into a triangular unit cell, shown in Fig. 5. The boundary conditions for this cell require that all its angles remain unchanged and all its sides remain straight throughout the deformation process. The NASTRAN finite-element model for the unit cell consists of a total of 55 elements, as shown in Fig. 6. The hoop stress, σ_R, in the resin in the vicinity of the strain gauge, shown in Fig. 5, was singled out from the finite-element calculations as the most important residual stress component.

4. Results and discussion

Residual strain build-up throughout the cure cycle was measured for the resin systems listed in Table II, and the results are shown in Figs 7 to 10. The measured final transverse strains, ϵ_R, in the glass rods of the apparatus and the residual hoop stresses, σ_R, in the resins, calculated from the finite-element analysis, are given in Table III. It is hard to compare the measured axial strains in the glass rods because of the uncertain locations of the axial strain gauges in the samples. Since the axial strains are of less significance to transverse cracking, they will only be mentioned for qualitative reference purposes. Table III also shows the critical stress intensity factor, K_c, and critical strain energy release rate, G_c, obtained from fracture toughness tests, the glass transition temperature, T_g, the thermal expansion coefficient, α, from TMA, and Young's modulus, E, and yield stress, σ_y, from compression tests.

4.1. Residual stress

4.1.1. System 6010/972

For the System 6010/972 (see Fig. 7), the initial resin shrinkage during curing was moderated with a slight exotherm-induced (120° C) expansion resulting in a small residual stress in the resin. During the post-cure, however, an additional amount of residual stress was built up due to resin shrinkage. After the sample had cooled to room temperature, the final residual hoop strain, ϵ_R, was approximately 1.50×10^{-4}. The residual hoop stress, σ_R, in the resin was calculated by using the NASTRAN finite-element computer program and found to be approximately 36 MPa in tension.

4.1.2. System 6010/906

The System 6010/906 (see Fig. 8) gelled at approximately 80° C during the initial heating. As the temperature rose above the gel point to reach the scheduled cure temperature (150° C), the thermally induced expansion of the gel overcame the subsequent resin shrinkage resulting in a net tensile strain in the glass rod. The final residual strain in the glass rod was approximately 7.5×10^{-5} corresponding to a tensile residual stress of 18 MPa in the resin.

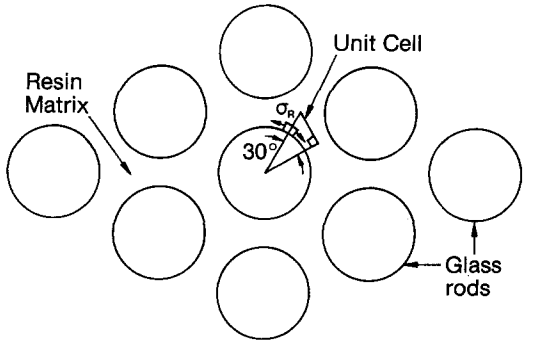

Figure 5 Cross-section of a hexagonal array of glass rods embedded in the resin matrix showing the repeated unit cell and the resin hoop stress, σ_R.

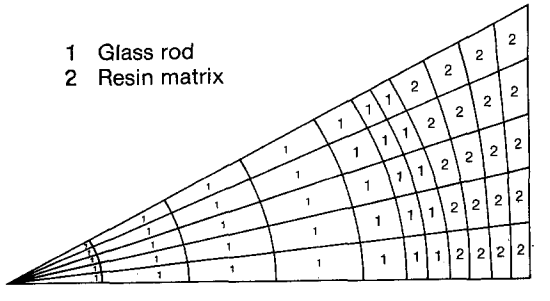

Figure 6 NASTRAN finite-element model of a unit cell for the calculation of stress field induced by the thermal misfit betweeen glass rod and resin.

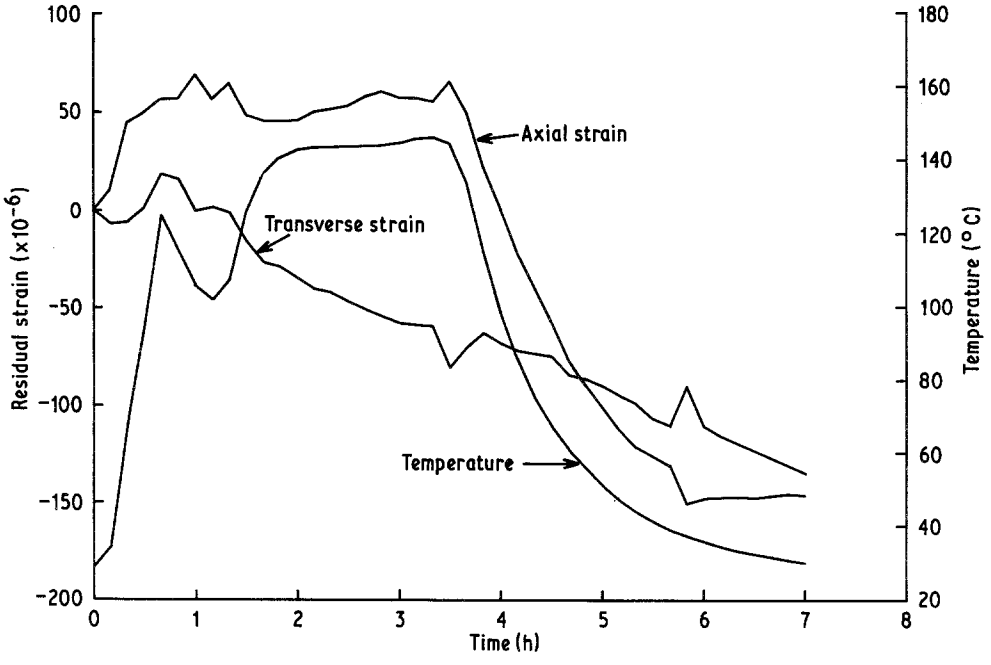

Figure 7 Residual strain build-up for glass rods in the resin System 6010/972.

4.1.3. System 6010/HY 917

In another system, 6010 epoxy resin was cured with HY 917, an anhydride hardener, (see Fig. 9) at 150° C for 3 h. Although gelation was visually observed to start at approximately 120° C during the initial heating, further resin shrinkage developed during curing of the resin. The final residual strain on the central glass rod was 3.00×10^{-4}. The residual stress in the resin was calculated to be 71.5 MPa in tension. The large temperature span in the curing cycle seemed to contribute to the large measured residual strain.

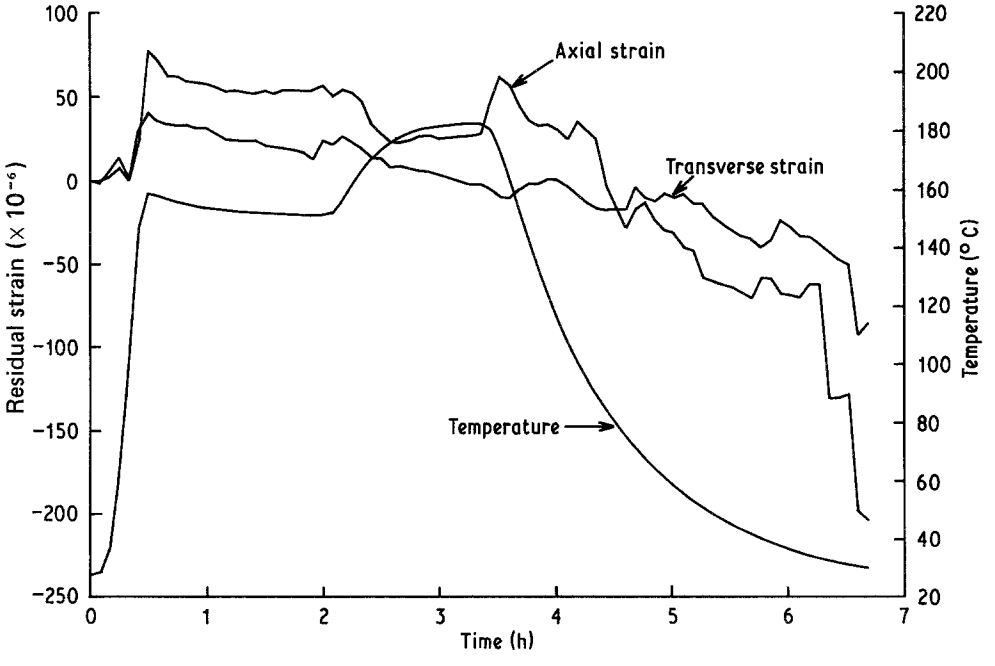

Figure 8 Residual strain build-up for glass rods in the resin System 6010/906.

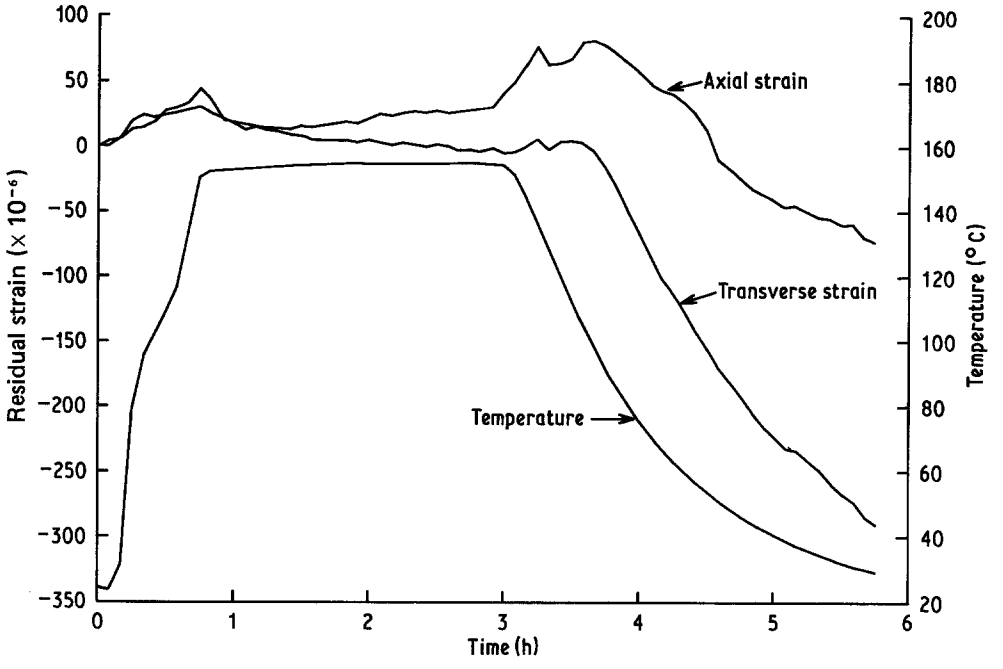

Figure 9 Residual strain build-up for glass rods in the resin System 6010/HY 917.

4.1.4. System 6010/PACM 20/972

In view of the experimental results of stress in the System 6010/HY 917, attempts were made to lower the gel point of the resin system in order to lower the residual stress level. Two resin systems were investigated, curing 6010 with a mixture of 972 and different ratios of DuPont PACM 20, a low-temperature curing agent (hydrogenated MDA). It was speculated that PACM 20 would advance the reaction of resin at relatively low initial curing temperature (80° C) to minimize the resin shrinkage induced by chemical reaction dur-

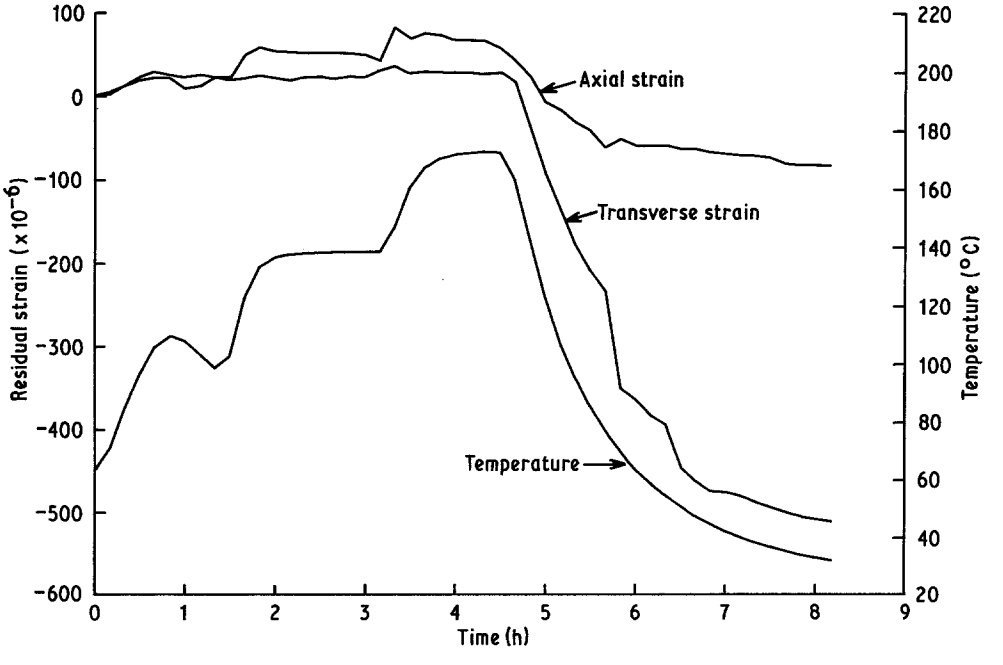

Figure 10 Residual strain build-up for glass rods in the resin System 6010/PACM 20/972.

TABLE III Material properties of the resin systems investigated

Epoxy resin hardener system	Measured residual strain, ϵ_R ($\times 10^{-6}$)	Resin residual stress, σ_R (MPa)	Critical stress intensity factor, K_c (MN m$^{-3/2}$)	Critical strain energy release rate, G_c (J m^{-2})	Glass transition temperature, T_g (°C)	Thermal expansion coefficient, α, below/above T_g ($\times 10^{-5}$ C^{-1})	Young's modulus E (GPa)	Yield stress, σ_y (MPa)	Residual stress due to thermal misfit below T_g, σ'_T (MPa)	Residual stress due to thermal misfit above T_g, σ''_T (MPa)	Total residual stress due to thermal misfit, σ_T (MPa)
6016/972	−150	36	0.72	142	90	5.0/10.0	3.61	116	15	29	44
6010/906	−72	18	0.52	84	150	6.0/14.0	3.21	115	33 (14.5*)	17	50
6010/HY 917	−300	71.5	0.68	144	110	6.5/18.0	3.23	126	24	33	57
6010/PACM 20/972	−500	119	0.83	249	156	7.6/16.0	2.76	109	37	12	49

* Calculated by considering thermal misfit due to a temperature change from 80° C to room temperature (25° C).

ing the later post-cure. The test to measure the residual stress in this system with 972/PACM 20 weight ratio 4:1 was not successful due to separation of the transverse strain gauge leads. The other system with 972/PACM 20 (weight ratio 2.3:1) (see Fig. 10), gelled at 80° C with an exotherm at 110° C. The final residual strain of this system was 5.00×10^{-4} which corresponded to a residual stress of 119 MPa in the resin. This was considerably higher than the residual stress of 36 MPa observed earlier in the System 6010/972. The application of the low temperature curing agent, PACM 20, did not lower the residual stress level as originally speculated.

4.2. Sources of the residual stress

In order to account for the contribution to the final residual stress in the resin due to thermal mismatch between the resin and the glass rod, finite element calculations were carried out using the measured T_g and α values from Table III with the assumption of zero stress relaxation. The residual stress, σ'_T, generated by a temperature change from T_g to room temperature (25° C), and the residual stress, σ''_T, at room temperature resulting from the strain generated by a temperature change from the maximum post-cure temperature to T_g are given in Table III. Note that σ''_T defined here is not the residual stress developed at T_g. Instead it is the stress component at room temperature induced by the thermal misfit strain which is accumulated above T_g and which assumed to be unrelaxed during the cooling process. The net residual stress σ_T, also included in Table III, caused by the total temperature change from the post-cure temperature to room temperature, is given by the sum of σ'_T and σ''_T.

As can be seen from Table III, σ'_T alone cannot account for all the measured residual stresses, σ_R, for Systems 6010/972, 6010/HY 917 and 6010/PACM 20/972. This indicates that the thermal misfits above T_g for these systems were not totally relaxed during curing. For Systems 6010/HY 917 and 6010/PACM 20/972, even their σ_T values, the maximum residual stresses possibly developed from a thermal misfit, are smaller than their individual measured σ_R values. The discrepancies indicate the existence of another source of residual stress: resin shrinkage induced by chemical reaction. Although the System 6010/972 had a calculated σ_T value larger than σ_R, the actual residual stress in excess of σ'_T can still be generated by both thermal misfit above T_g and chemical reaction.

The System 6010/906 has a measured residual stress, σ_R, lower than the calculated σ'_T. This system cured with a relatively large amount of accelerator 064 was probably almost fully reacted, immediately after gelation at 80° C. If we consider a thermal misfit caused by a temperature change from 80° C to room temperature, the residual stress so induced is 14.5 MPa, which is close to the corresponding measured value of 18 PMa. This seems to suggest that the System 6010/906 had a more or less fixed structure near its gel point during curing.

Several interesting conclusions can be drawn from the above results.

(a) Contrary to the common belief that all stresses would be relieved above T_g, the residual stress was found to build up as a direct result of the thermal mismatch above T_g. The elastic modulus of the resin above T_g is usually about one order of magnitude lower than that below T_g. This means that the unrelaxed elastic residual strain above T_g may be large, but the residual stress will remain low. This could be deduced from the usually small residual stress in the resin above T_g observed in out tests. Although the large strain above T_g corresponds to a small value of stress, after the material is cooled below T_g the unrelaxed portion of this strain will result in a large stress because of the large increase in stiffness of the resin.

(b) It seems that during the curing process the temperature at which the chemical reaction is nearly complete heavily influences the final residual stress level. If this temperature level is above T_g the residual stress produced by thermal mismatch alone can be very large, resulting from the large thermal expansion coefficient above T_g. From the point of view of reducing the residual stress, it is desirable to lower this temperature level.

(c) As can be seen from Table III, the residual stresses in the resin systems observed in our study were generally high. These results represent the residual stresses in unidirectional laminates containing a hexagonal array of glass-fibre rods (65 vol%) embedded in epoxy resins. In a real composite, however, the distribution of fibres is far from uniform. There definitely exist regions with fibre contents much higher than the overall average fibre content. In such regions the residual stresses are likely to be much higher than those measured from our glass rod–epoxy samples at 65 vol% fibre content. It would not be unreasonable to

speculate that such high stresses can cause damage, such as short cracking, to occur in the laminate. The regions of high fibre content can, therefore, be preferential sites for crack initiation and propagation.

4.3. Other material variables

The fracture-toughness results listed in Table III represent the individual, fundamental fracture properties of the resins in this investigation. The toughening effect from adding PACM 20 to the System 6010/972, was shown by the improved fracture-toughness measured on the System 6010/PACM 20/972. The relationship between the fracture-toughness and the curing cycle of the resins was not immediately obvious from the results of our study. However, fracture-toughness of the resin can be optimized by controlling certain variables such as the hardener content and the curing schedule. The correlation between the fracture-toughness and the yield stress, a possible energy absorbing mechanism, was not conclusive. The system 6010/PACM 20/972, nevertheless, had lower σ_y value than the System 6010/972, demonstrating the increased flexibility of the resin System 6010/972 with added PACM 20.

From the point of view of transverse cracking resistance, a desired resin system for composites should have a high fracture-toughness and a low residual stress. These studies have shown that a tough resin system may have a very high residual stress build-up in the laminate which, after all, may not be desirable. When selecting resins for composite applications, one, therefore, has to be careful not to improve either one of the material variables at the expense of the other. The unique testing technique used in this work for measuring residual stress in the resin was quite effective in characterizing the residual stresses. Moreover, valuable information has been collected through these tests concerning residual stress build-up characteristics during cure and possible ways of reducing such build-up.

5. Conclusions

In this study, two important material properties of resins, the residual stress and the fracture-toughness, which contribute to the transverse cracking process of composites, were investigated. From the view-point of optimization of composite material properties, resins should be screened at least for these two properties.

The new testing technique for measuring the residual stress in the resin in the laminate used in this work has been proven to be effective. In fact, it is also applicable to other fibre–resin systems in addition to the glass-fibre–epoxy systems studied here. The measurements performed on several resin systems have shown that the residual stress in the resins can be severe and that the resin curing characteristics heavily influence the final residual stress in the resin.

An interesting point observed in this study was that the residual stress built up as a direct result of the thermal mismatch above T_g. Although the large strain above T_g corresponds to a small value of stress, after the material is cooled below T_g the unrelaxed portion of this strain will result in a large stress because of the large increase in stiffness of the resin.

High resin fracture-toughness and low resin residual stress are the conditions desired for the laminate to resist transverse cracking. Although this ideal combination was not realized for the resin systems in our study, it should be achievable once the curing cycle as well as the resin formulation are propertly adjusted. Although further work still remains to be done in order to develop a more detailed description of micro-failure mechanisms, the current study does indicate an approach to the improvement of transverse cracking resistance in composites.

References

1. K. W. GARRETT and J. E. BAILEY, *J. Mater. Sci.* **12** (1977) 157.
2. A. PARVIZI, K. W. GARRETT and J. E. BAILEY, *ibid.* **13** (1978) 195.
3. A. PARVIZI and J. E. BAILEY, *ibid.* **13** (1978) 2131.
4. J. E. BAILEY, P. T. CURTIS and A. PARVIZI, *Proc. Roy. Soc.* **A366** (1979) 599.
5. M. G. BADER, J. E. BAILEY, P. T. CURTIS and A. PARVIZI, Proceedings of the 3rd International Symposium on the Mechanical Behaviour of Materials, Cambridge, UK (Pergamon Press, Oxford, UK, Elmsford, New York, 1980), Vol. 3, 20–24 August, 1979, p. 227.
6. A. S. D. WANG and F. W. CROSSMAN, *J. Comp. Mater. Suppl.* **14** (1980) 71.
7. F. W. CROSSMAN, W. J. WARREN, A. S. D. WANG and G. E. LAW, Jr, *ibid.* **14** (1980) 88.
8. R. M. CHRISTENSEN and J. A. RINDE, *Polymer Eng. Sci.* **19** (1979) 506.
9. K. W. GARRET and J. E. BAILEY, *J. Mater. Sci.* **12** (1977) 2189.
10. J. E. BAILEY and A. PARVIZI, *ibid.* **16** (1981) 649.

11. S. K. GAGGAR and L. J. BROUTMAN, *Polymer Eng. Sci.* **16** (1976) 537.
12. I. M. DANIEL, in "Composite Materials" Vol. 2, edited by L. J. Broutman and R. H. Krock (Academic Press, New York, 1974) Chap. 10.
13. B. CUNNINGHAM, J. P. SARGENT, and K. H. G ASHBEE, *J. Mater. Sci.* **16** (1981) 620.
14. J. F. KNOTT, "Fundamentals of Fracture Mechanics" (Halsted Press, New York, 1973) p. 130.
15. D. BROEK, "Elementary Engineering Fracture Mechanics" (Sijthoff and Noordhoff, Amsterdam, 1978) p. 166.

Received 2 September
and accepted 15 December 1981